

# Fundamental limits on the rate of bacterial cell division

<sup>3</sup> **Nathan M. Belliveau<sup>†, 1</sup>, Griffin Chure<sup>†, 2, 3</sup>, Christina L. Hueschen<sup>4</sup>, Hernan G.  
<sup>4</sup> Garcia<sup>5</sup>, Jané Kondev<sup>6</sup>, Daniel S. Fisher<sup>7</sup>, Julie Theriot<sup>1, 8</sup>, Rob Phillips<sup>2, 9, \*</sup>**

\*For correspondence:

<sup>†</sup>These authors contributed equally to this work

<sup>5</sup> <sup>1</sup>Department of Biology, University of Washington, Seattle, WA, USA; <sup>2</sup>Division of  
<sup>6</sup> Biology and Biological Engineering, California Institute of Technology, Pasadena, CA,  
<sup>7</sup> USA; <sup>3</sup>Department of Applied Physics, California Institute of Technology, Pasadena, CA,  
<sup>8</sup> USA; <sup>4</sup>Department of Chemical Engineering, Stanford University, Stanford, CA, USA;  
<sup>9</sup> <sup>5</sup>Department of Molecular Cell Biology and Department of Physics, University of  
<sup>10</sup> California Berkeley, Berkeley, CA, USA; <sup>6</sup>Department of Physics, Brandeis University,  
<sup>11</sup> Waltham, MA, USA; <sup>7</sup>Department of Applied Physics, Stanford University, Stanford, CA,  
<sup>12</sup> USA; <sup>8</sup>Allen Institute for Cell Science, Seattle, WA, USA; <sup>9</sup>Department of Physics,  
<sup>13</sup> California Institute of Technology, Pasadena, CA, USA; \*Contributed equally

<sup>14</sup> 

---

<sup>15</sup> **Abstract** This will be written next

<sup>16</sup> 

---

## <sup>17</sup> Uptake of Nutrients

<sup>18</sup> In order to build new cellular mass, the molecular and elemental building blocks must be scav-  
<sup>19</sup> enged from the environment in different forms. Carbon, for example, is acquired via the transport  
<sup>20</sup> of carbohydrates and sugar alcohols with some carbon sources receiving preferential treatment  
<sup>21</sup> in their consumption (?). Phosphorus, sulfur, and nitrogen, on the other hand, are harvested pri-  
<sup>22</sup> marily in the forms of inorganic salts, namely phosphate, sulfate, and ammonia (??????). All of  
<sup>23</sup> these compounds have different permeabilities across the cell membrane and most require some  
<sup>24</sup> energetic investment either via ATP hydrolysis or through the proton electrochemical gradient to  
<sup>25</sup> bring the material across the hydrophobic cell membrane. Given the diversity of biological trans-  
<sup>26</sup> port mechanisms and the vast number of inputs needed to build a cell, we begin by considering  
<sup>27</sup> transport of some of the most important cellular ingredients: carbon, nitrogen, oxygen, hydrogen,  
<sup>28</sup> phosphorus, and sulfur.

<sup>29</sup> The elemental composition of *E. coli* has received much quantitative attention over the past  
<sup>30</sup> half century (????), providing us with a starting point for estimating the copy numbers of various  
<sup>31</sup> transporters. While there is some variability in the exact elemental percentages (with different un-  
<sup>32</sup> certainties), we can estimate that the dry mass of a typical *E. coli* cell is  $\approx$  45% carbon (BNID: 100649,  
<sup>33</sup> ?),  $\approx$  15% nitrogen (BNID: 106666, ?),  $\approx$  3% phosphorus (BNID: 100653, ?), and 1% sulfur (BNID:  
<sup>34</sup> 100655, ?). In the coming paragraphs, we will engage in a dialogue between back-of-the-envelope  
<sup>35</sup> estimates for the numbers of transporters needed to facilitate these chemical stoichiometries and  
<sup>36</sup> the experimental proteomic measurements of the biological reality. Such an approach provides  
<sup>37</sup> the opportunity to test if our biological knowledge is sufficient to understand the scale at which  
<sup>38</sup> these complexes are produced. Specifically, we will make these estimates considering a modest  
<sup>39</sup> doubling time of 5000 s, a growth rate of  $\approx$  0.5 hr<sup>-1</sup>, the range in which the majority of the experi-  
<sup>40</sup> mental measurements reside.

**41 Nitrogen Transport**

42 Before we begin our back-of-the-envelope estimations, we must address which elemental sources  
 43 must require proteinaceous transport, meaning that the cell cannot acquire appreciable amounts  
 44 simply via diffusion from the membrane. The permeability of the lipid membrane to a large num-  
 45 ber of solutes has been extensively characterized over the past century. Large, polar molecular  
 46 species (such as various sugar molecules, sulfate, and phosphate) have low permeabilities while  
 47 small, non-polar compounds (such as oxygen, carbon dioxide, and ammonia) can readily diffuse  
 48 across the membrane. Ammonia, a primary source of nitrogen in typical laboratory conditions, has  
 49 a permeability on par with water ( $\approx 10^5$  nm/s, BNID:110824 ?). In particularly nitrogen-poor condi-  
 50 tions, *E. coli* expresses a transporter (AmtB) which appears to aid in nitrogen assimilation, though  
 51 the mechanism and kinetic details of transport is still a matter of debate (??). Beyond ammonia,  
 52 another plentiful source of nitrogen come in the form of glutamate, which has its own complex  
 53 metabolism and scavenging pathways. However, nitrogen is plentiful in the growth conditions ex-  
 54 amined in this work, permitting us to neglect nitrogen transport as a potential rate limiting process  
 55 in cell division in typical experimental conditions. We direct the reader to the supplemental infor-  
 56 mation for a more in-depth discussion of permeabilities and a series of calculations revealing that  
 57 active nitrogen transport can be neglected for the purposes of this article.

**58 Carbon Transport**

59 We begin our estimations with the most abundant element in *E. coli* by mass, carbon. Using  $\approx 0.3$   
 60 pg as the typical *E. coli* dry mass (BNID: 103904, ?), we estimate that  $\approx 10^{10}$  carbon atoms must be  
 61 brought into the cell in order to double all of the carbon-containing molecules (*Figure 1(A, top)*)).  
 62 Typical laboratory growth conditions, such as those explored in the aforementioned proteomic  
 63 data sets, provide carbon as a single class of sugar such as glucose, galactose, or xylose to name a  
 64 few. *E. coli* has evolved myriad mechanisms by which these sugars can be transported across the  
 65 cell membrane. One such mechanism of transport is via the PTS system which is a highly modu-  
 66 lar system capable of transporting a diverse range of sugars (?). The glucose-specific component  
 67 of this system transports  $\approx 200$  glucose molecules per second per transporter (BNID: 114686, ?).  
 68 Making the assumption that this is a typical sugar transport rate, coupled with the need to trans-  
 69 port  $10^{10}$  carbon atoms, we arrive at the conclusion that on the order of 1,000 transporters must  
 70 be expressed in order to bring in enough carbon atoms to divide in 5000 s, diagrammed in the  
 71 top panel of *Figure 1(A)*. This estimate, along with the observed average number of the PTS sys-  
 72 tem carbohydrate transporters present in the proteomic data sets (????), is shown in *Figure 1(A)*.  
 73 While we estimate 1500 transporters are needed with a 5000 s division time, we can abstract this  
 74 calculation to consider any particular growth rate given knowledge of the cell density and volume  
 75 as a function of growth rate and direct the reader to the SI for more information. As revealed  
 76 in *Figure 1(A)*, experimental measurements exceed the estimate by several fold, illustrating that  
 77 transport of carbon in to the cell is not rate limiting for cell division.

78 The estimate presented in *Figure 1(A)* neglects any specifics of the regulation of carbon trans-  
 79 port system and presents a data-averaged view of how many carbohydrate transporters are present  
 80 on average. Using the diverse array of growth conditions explored in the proteomic data sets, we  
 81 can explore how individual carbon transport systems depend on the population growth rate. In  
 82 *Figure 1(B)*, we show the total number of carbohydrate transporters specific to different carbon  
 83 sources. A striking observation, shown in the top-left plot of *Figure 1(B)*, is the constancy in the  
 84 expression of the glucose-specific transport systems. Additionally, we note that the total number  
 85 of glucose-specific transporters is tightly distributed  $\approx 10^4$  per cell, the approximate number of  
 86 transporters needed to sustain rapid growth of several divisions per hour, as indicated by the grey  
 87 shaded line. This illustrates that *E. coli* maintains a substantial number of complexes present for  
 88 transporting glucose which is known to be the preferential carbon source (??).

89 It is now understood that a large number of metabolic operons are regulated with dual-input  
 90 logic gates that are only expressed when glucose concentrations are low (mediated by cyclic-AMP

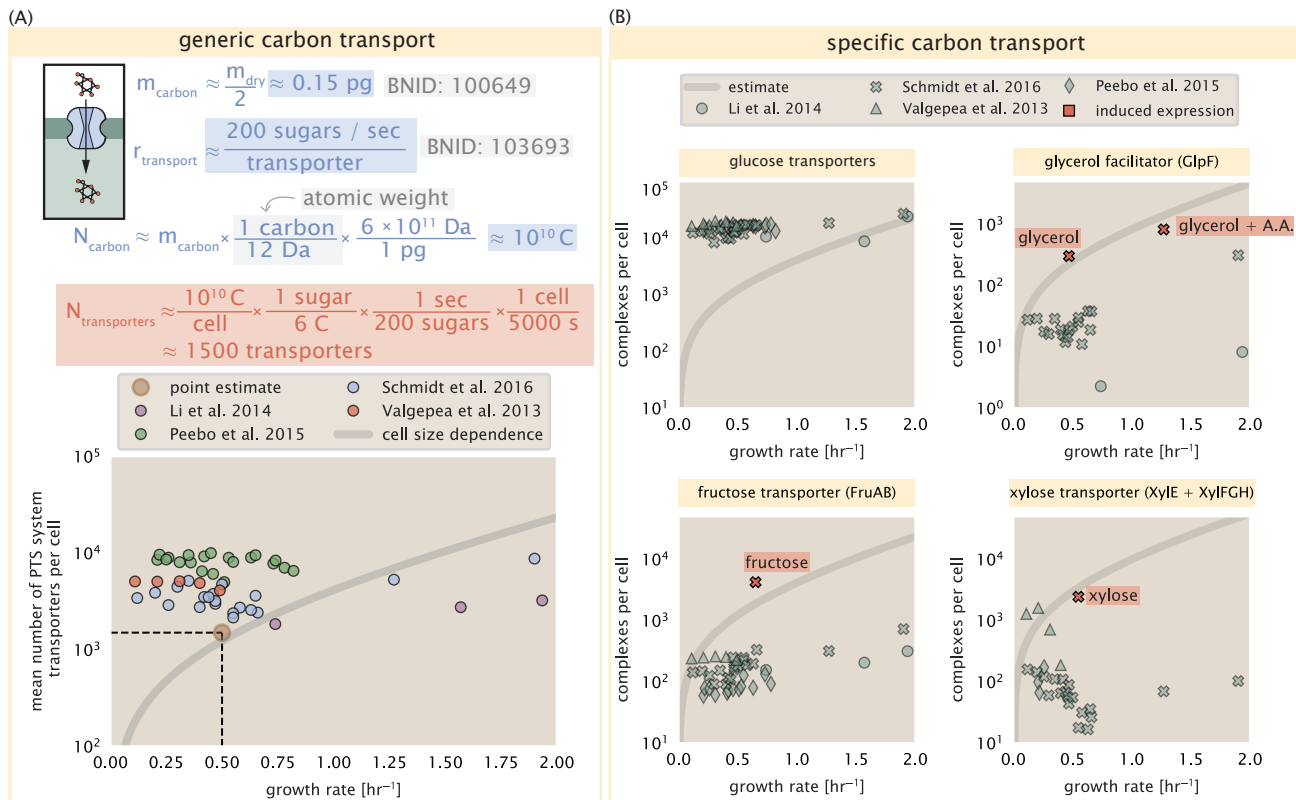


**Figure 1. The abundance of carbon transport systems across growth rates.** (A) A simple estimate for the minimum number of generic carbohydrate transport systems (top) assumes  $\approx 10^{10}$  C are needed to complete division, each transported sugar contains  $\approx 6$  C, and each transporter conducts sugar molecules at a rate of  $\approx 200$  per second. Bottom plot shows the estimated number of transporters needed at a growth rate of  $\approx 0.5$  per hr (light-brown point and dashed lines). Colored points correspond to the mean number of PTS system sugar transporters (complexes annotated with the Gene Ontology term GO:0009401) for different growth conditions across different published datasets. (B) The abundance of various specific carbon transport systems plotted as a function of the population growth rate. Red points and red-highlighted text indicate conditions in which the only source of carbon in the growth medium induces expression of the transport system. Grey line in (A) and (B) represents the estimated number of transporters per cell at a continuum of growth rates.

receptor protein CRP) and the concentration of other carbon sources are elevated (??). A famed example of such dual-input regulatory logic is in the regulation of the *lac* operon which is only natively activated in the absence of glucose and the presence of allolactose, an intermediate in lactose metabolism (?), though we now know of many other such examples (??). This illustrates that once glucose is depleted from the environment, cells have a means to dramatically increase the abundance of the specific transporter needed to digest the next sugar that is present. Several examples of induced expression of specific carbon-source transporters are shown in *Figure 1(B)*. Points colored in red (labeled by red text-boxes) correspond to growth conditions in which the specific carbon source (glycerol, xylose, or fructose) is present. These plots show that, in the absence of the particular carbon source, expression of the transporters is maintained on the order of  $\sim 10^2$  per cell. However, when induced, the transporters become highly-expressed and fall close to the predicted number of transporters needed to facilitate growth on that substrate alone, shown as a transparent grey line. Together, this generic estimation and the specific examples of induced expression suggest that transport of carbon across the cell membrane, while critical for growth, is not the rate-limiting step of cell division.

### **106 Phosphorus and Sulfur Transport**

We now turn our attention towards other essential elements, namely phosphorus and sulfur. Phosphorus is critical to the cellular energy economy in the form of high-energy phosphodiester bonds making up DNA, RNA, and the NTP energy pool as well as playing a critical role in the post-translational modification of proteins and defining the polar-heads of lipids. In total, phosphorus makes up  $\approx 3\%$  of the cellular dry mass which in typical experimental conditions is in the form of inorganic phosphate. The cell membrane has remarkably low permeability to this highly-charged and critical molecule, therefore requiring the expression of active transport systems. In *E. coli*, the proton electrochemical gradient across the inner membrane is leveraged to transport inorganic phosphate into the cell (?). Proton-solute symporters are widespread in *E. coli* (??) and can have rapid transport rates of 50 to 100 molecules per second for sugars and other solutes (BNID: 103159; 111777, ?). As a more extreme example, the proton transporters in the F<sub>1</sub>-F<sub>0</sub> ATP synthase, which leverage the proton electrochemical gradient for rotational motion, can shuttle protons across the membrane at a rate of  $\approx 1000$  per second (BNID: 104890; 103390, (?)). In *E. coli* the PitA phosphate transport system has been shown to be very tightly coupled with the proton electrochemical gradient with a 1:1 proton:phosphate stoichiometric ratio (??). Taking the geometric mean of the aforementioned estimates gives a plausible rate of phosphate transport on the order of 300 per second. Illustrated in *Figure 2(A)*, we can estimate that  $\approx 150$  phosphate transporters are necessary to maintain an  $\approx 3\%$  dry mass with a 5000 s division time. This estimate is again satisfied when we examine the observed copy numbers of PitA in proteomic data sets (plot in *Figure 2(A)*). While our estimate is very much in line with the observed numbers, we emphasize that this is likely a slight overestimate of the number of transporters needed as there are other phosphorous scavenging systems, such as the ATP-dependent phosphate transporter Pst system which we have neglected.

Satisfied that there are a sufficient number of phosphate transporters present in the cell, we now turn to sulfur transport as another potentially rate limiting process. Similar to phosphate, sulfate is highly-charged and not particularly membrane permeable, requiring active transport. While there exists a H<sup>+</sup>/sulfate symporter in *E. coli*, it is in relatively low abundance and is not well characterized (?). Sulfate is predominantly acquired via the ATP-dependent ABC transporter CysUWA system which also plays an important role in selenium transport (??). While specific kinetic details of this transport system are not readily available, generic ATP transport systems in prokaryotes transport on the order of 1 to 10 molecules per second (BNID: 109035, ?). Combining this generic transport rate, measurement of sulfur comprising 1% of dry mass, and a 5000 second division time yields an estimate of  $\approx 1000$  CysUWA complexes per cell (*Figure 2(B)*). Once again, this estimate is in notable agreement with proteomic data sets, suggesting that there are sufficient transporters present to acquire the necessary sulfur. In a similar spirit of our estimate of phosphorus transport,

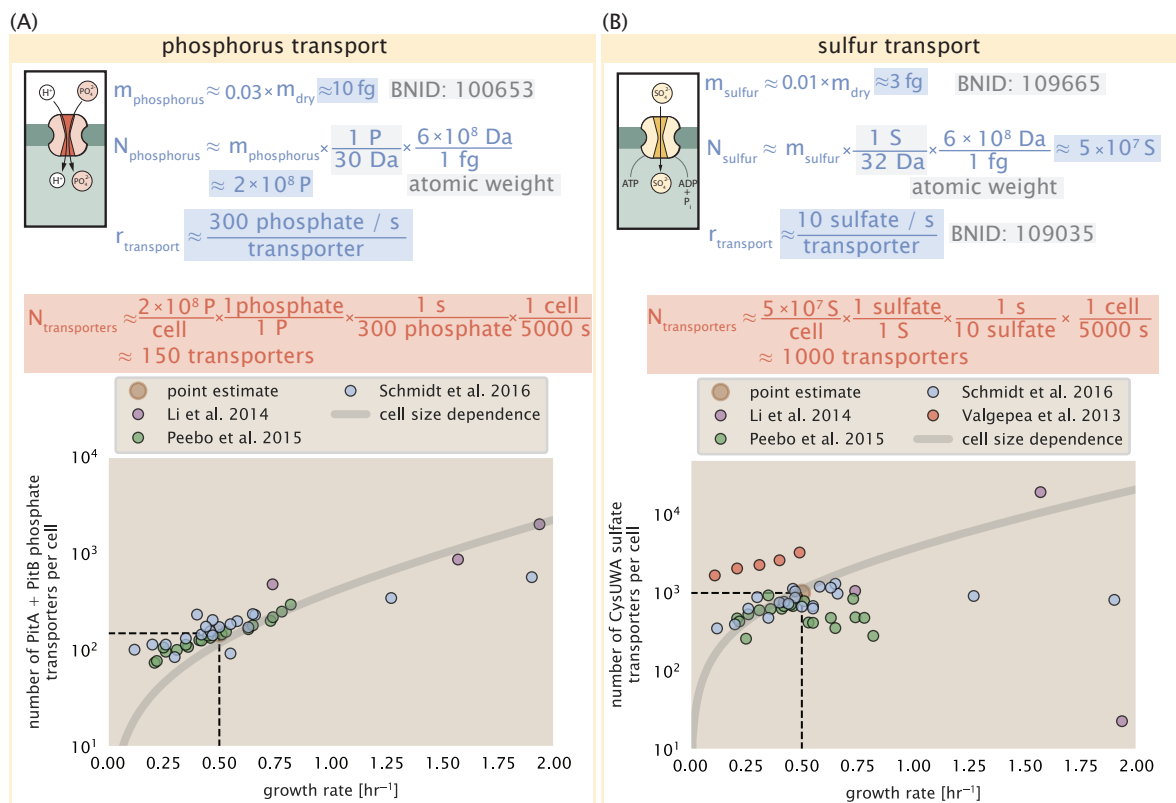


**Figure 2. Estimates and measurements of phosphate and sulfate transport systems as a function of growth rate.** (A) Estimate for the number of PitA phosphate transport systems needed to maintain a 3% phosphorus *E. coli* dry mass. Points in plot correspond to the total number of PitA transporters per cell. (B) Estimate of the number of CysUWA complexes necessary to maintain a 1% sulfur *E. coli* dry mass. Points in plot correspond to average number of CysUWA transporter complexes that can be formed given the transporter stoichiometry  $[\text{CysA}]_2[\text{CysU}][\text{CysW}][\text{Sbp/CysP}]$ . Grey line in (A) and (B) represents the estimated number of transporters per cell at a continuum of growth rates.

141 we emphasize that this is likely an overestimate of the number of necessary transporters as we  
142 have neglected other sulfur scavenging systems that are in lower abundance.

### 143 **Limits on Transporter Expression**

144 So which, if any, of these processes may be rate limiting for growth? As suggested by **Figure 1**  
145 (B), induced expression can lead to an order-of-magnitude (or more) increase in the amount of  
146 transporters needed to facilitate transport. Thus, if acquisition of nutrients was the limiting state  
147 in cell division, could expression simply be increased to accommodate faster growth? A way to  
148 approach this question is to compute the amount of space in the bacterial membrane that could  
149 be occupied by nutrient transporters. Considering a rule-of-thumb for the surface area of *E. coli* of  
150 about  $6 \mu\text{m}^2$  (BNID: 101792, ?), we expect an areal density for 1000 transporters to be approximately  
151 200 transporters/ $\mu\text{m}^2$ . For a typical transporter occupying about  $50 \text{ nm}^2/\text{dimer}$ , this amounts to  
152 about only 1 percent of the total inner membrane (?). In addition, bacterial cell membranes typically  
153 have densities of  $10^5$  proteins/ $\mu\text{m}^2$  (?), implying that the cell could accommodate more transporters  
154 of a variety of species if it were rate limiting. As we will see in the next section, however, occupancy  
155 of the membrane can impose other limits on the rate of energy production.

### 156 **Protein synthesis**

157 Lastly, we turn our attention to the process of translation. So far our estimates have led to protein  
158 copy numbers that are consistent with the proteomic data, or even in excess of what might be

needed for each task under limiting growth conditions. Even in our example of *E. coli* grown under different carbohydrate sources (**Figure 1(B)**), it becomes clear cells can utilize alternative carbon sources by inducing the expression of additional membrane transporters and enzymes. Optimal resource allocation and the role of ribosomal proteins have been an area of intense quantitative study over the last decade by Hwa and others (??). From the perspective of limiting growth, our earlier estimate of rRNA highlighted the necessity for multiple copies of rRNA genes in order to make enough rRNA, suggesting the possibility that synthesis of ribosomes might be rate limiting. While the transcriptional demand for the ribosomal proteins is substantially lower than rRNA genes, since proteins can be translated from relatively fewer mRNA, other ribosomal proteins like the translation elongation factor EF-Tu also present a substantial burden. For EF-Tu in particular, it is the most highly expressed protein in *E. coli* and is expressed from multiple gene copies, tufA and tufB.

To gain some intuition of how translation may set the speed limit for bacterial growth, we consider the total number of peptide bonds that must be synthesized,  $N_{AA}$ . Noting that cell mass grows exponentially [GC: Citation Here], we can compute the number of amino acids to be polymerized as

$$N_{AA} = \frac{r_t R}{\lambda}, \quad (1)$$

where  $\lambda$  is the cell growth rate in  $s^{-1}$ ,  $r_t$  is the maximum translation rate in amino acids per second, and  $R$  is the average ribosome copy number per cell. Knowing the number of peptide bds to be formed permits us to compute the translation-limited growth rate as

$$\lambda_{\text{translation-limited}} = \frac{r_t R}{N_{AA}}. \quad (2)$$

Alternatively, since  $N_{AA}$  is related to the total protein mass through the molecular weight of each protein, we can also consider the growth rate in terms of the fraction of the total proteome mass that is dedicated to ribosomal protein mass. By making the approximation that an average amino acid has a molecular weight of 110 Da (see **Figure 3(A)**), we can rewrite the growth rate as,

$$\lambda_{\text{translation-limited}} \approx \frac{r_t}{L_R} \Phi_R, \quad (3)$$

where  $L_R$  is the total length in amino acids that make up a ribosome, and  $\Phi_R$  is the ribosomal mass fraction. This is plotted as a function of ribosomal fraction  $\Phi_R$  in **Figure 3(A)**, where we take  $L_R \approx 7500$  aa, corresponding to the length in amino acids for all ribosomal subunits of the 50S and 30S complex (BNID: 101175, (?)). This formulation assumes that the cell can transcribe the required amount of rRNA, which appears reasonable for *E. coli*, allowing us to consider the inherent limit on growth set by the ribosome.

The growth rate defined by Equation 3 reflects mass-balance under steady-state growth and has long provided a rationalization to the apparent linear increase in *E. coli*'s ribosomal content as a function of growth rate (??). For our purposes, there are several important consequences of this trend. Firstly, we note there is a maximum growth rate of  $\lambda \approx 6hr^{-1}$ , or doubling time of about 7 minutes (dashed line). This growth rate can be viewed as an inherent maximum growth rate due to the need for the cell to double the cell's entire ribosomal mass. Interestingly, this limit is independent of the absolute number of ribosomes and is simply given by time to translate an entire ribosome,  $L_R/r_t$ . As shown in **Figure 3(B)**, we can reconcile this with the observation that in order to double the average number of ribosomes, each ribosome must produce a second ribosome. Unlike DNA replication or rRNA transcription, this is a process that cannot be parallelized.

For reasonable values of  $\Phi_R$ , between about 0.1 - 0.3 (?), the maximum growth rate is in line with experimentally reported growth rates around  $0.5 - 2 hr^{-1}$ . Importantly, in order for a cell to scale this growth limit set by  $\Phi_R$ , cells *must* increase their ribosomal abundance. This can be achieved by either synthesizing more ribosomes or reducing the fraction of non-ribosomal proteins. Reduction of non-ribosomal proteins is not a straightforward task since (as we have found throughout our

203 estimates) doubling a cell requires many other enzymes and transporters. Increasing the absolute  
 204 ribosomal abundance for the case of *E. coli* is limited by the number of rRNA operons.

### 205 **Multiple replication forks help bias ribosome abundance.**

206 *E. coli* cells grow by a so-called "adder" mechanism, whereby cells add a constant volume with  
 207 each cell division (?). In conjunction with this, additional rounds of DNA replication are triggered  
 208 when cells reach a critical volume per origin of replication (**Figure 4(A)**). This leads to the classically-  
 209 described exponential increase in cell size with growth rate ????. However, the mechanism behind  
 210 growth rate control has remained elusive and has only been described at a phenomenological  
 211 level. In the context of maximizing growth rate, it is notable that the majority of ribosomal pro-  
 212 teins and rRNA operons are found closer to the DNA origin. Given that cells must increase their  
 213 total gene dosage of rRNA operons at faster growth rates, and the intimate relationship between  
 214 ribosomal content and growth rate considered above, this raises the possibility that the increase  
 215 in chromosomal content might simply be a means for the cell to tune biosynthesis according to its  
 216 physiological state and the nutrient availability in its environment.

217 While an increase in transcription has been observed for genes closer to the origin in rapidly  
 218 growing *E. coli* (?), we were unaware of such characterization at the proteomic level. In order to see  
 219 whether there is a relative increase in protein expression for genes closer to the origin at faster  
 220 growth, we calculated a running boxcar average (500 kbp window) of protein copy number as a  
 221 function of each gene's transcriptional start site (**Figure 4(B)**). While absolute protein copy numbers  
 222 can vary substantially across the chromosome, we indeed observe a bias in expression under fast  
 223 growth conditions (dark blue), showing the result. The dramatic change in protein copy number  
 224 near the origin is primarily due to the increase in ribosomal protein expression. This trend is in  
 225 contrast to slower growth conditions (yellow) where the average copy number is more uniform  
 226 across the length of the chromosome.

227 If ribosomal genes (rRNA and ribosomal proteins) are being synthesized at their maximal rate  
 228 according to the rRNA gene dosage, we can make two related hypotheses about how their ribo-  
 229 some abundance should vary with chromosomal content. First, the ribosomal protein fraction  
 230 should increase in proportion to the average ratio of DNA origins to DNA termini ( $\langle \# \text{ ori} \rangle / \langle \# \text{ ter} \rangle$   
 231 ratio). This is a consequence of the skew in DNA dosage as cells grow faster. The second hypothe-  
 232 sis is that the absolute number of ribosomes should increase with the number of DNA origins ( $\langle \# \text{ ori} \rangle$ ), since this will reflect the total gene dosage at a particular growth condition.

233 In order to test each of these expectations we considered the experimental data from ?, which  
 234 inferred these parameters for cells under nutrient-limited growth. The ratio  $\langle \# \text{ ori} \rangle / \langle \# \text{ ter} \rangle$  de-  
 235 pends on how quickly chromosomes are replicated relative the cell's doubling time  $\tau$  and is given  
 236 by  $2^{\tau_C/\tau}$ . Here  $\tau_C$  is the time taken to replicate *E. coli*'s chromosome, referred to as the C period of  
 237 cell division. In **Figure 4(C)** we plot the measured  $\tau_C$  versus  $\tau$  (computed as  $\tau = \log(2)/\lambda$ ), with data  
 238 points in red corresponding to *E. coli* strain MG1655, and blue to strain NCM3722. ? also measured  
 239 the total RNA to protein ratio which reflects ribosomal abundance and we show that data along  
 240 with other recent measurements from ???. Indeed, we find that the ribosomal fraction increases  
 241 with  $\langle \# \text{ ori} \rangle / \langle \# \text{ ter} \rangle$  (**Figure 4(C)**). We note a systematic difference in the relative abundances from  
 242 ? and ? that was inconsistent with a number of other measurements of total RNA-to-protein ratios  
 243 ( $\approx \Phi_R \times 2.1$  ?) and only show the data from ? and ? for relative ribosome abundances (see sup-  
 244 plemental section XX for a more complete discussion). For the data shown, the ribosomal fraction  
 245 doesn't increase as much at higher  $\langle \# \text{ ori} \rangle / \langle \# \text{ ter} \rangle$ . Since several rRNA operons are actually located  
 246 approximately half-way between the origin and terminus, the trend may in part be a consequence  
 247 of a diminishing increase in rRNA gene dosage at higher  $\langle \# \text{ ori} \rangle / \langle \# \text{ ter} \rangle$  ratios.

248 We can similarly estimate  $\langle \# \text{ ori} \rangle$ , which depends on how often replication forks are initiated  
 249 per cell cycle. This is given by the number of overlapping cell cycles,  $2^{\tau_{\text{cyc}}/\tau}$ , where  $\tau_{\text{cyc}}$  refers to the  
 250 total time of chromosome replication and cell division. **Figure 4(E)** shows the associated data from  
 251 ?, which we use to estimate  $\langle \# \text{ ori} \rangle$  for each growth condition of the proteomic data. In agreement

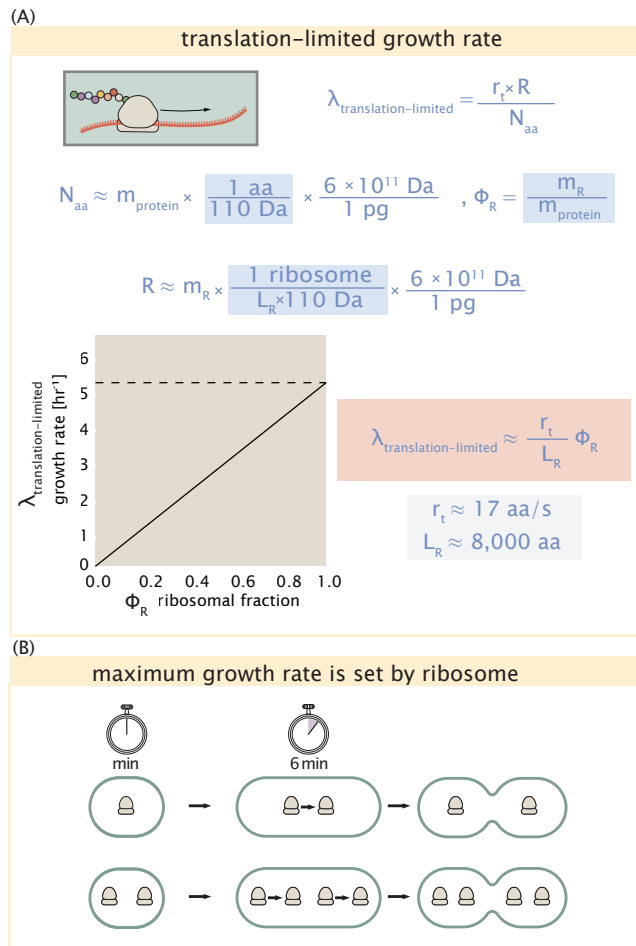


**Figure 3. Translation-limited growth rate.** (A) Here we consider the translation-limited growth as a function of ribosomal fraction. By mass balance, the time required to double the entire proteome ( $N_{AA} / r_t$ ) sets the translation-limited growth rate,  $\lambda_{\text{translation-limited}}$ . Here  $N_{aa}$  is effectively the number of peptide bonds that must be translated,  $r_t$  is the translation elongation rate, and  $R$  is the number of ribosomes. This can also be re-written in terms of the ribosomal mass fraction  $\Phi_R = m_R / m_{\text{protein}}$ , where  $m_R$  is the total ribosomal mass and  $m_{\text{protein}}$  is the mass of all proteins in the cell.  $L_R$  refers to the summed length of the ribosome in amino acids.  $\lambda_{\text{translation-limited}}$  is plotted as a function of  $\Phi_R$  (solid line). (B) The dashed line in part (A) identifies a maximum growth rate that is set by the ribosome. Specifically, this growth rate corresponds to the time required to translate an entire ribosome,  $L_R / r_t$ . This is a result that is independent of the number of ribosomes in the cell as shown schematically here.

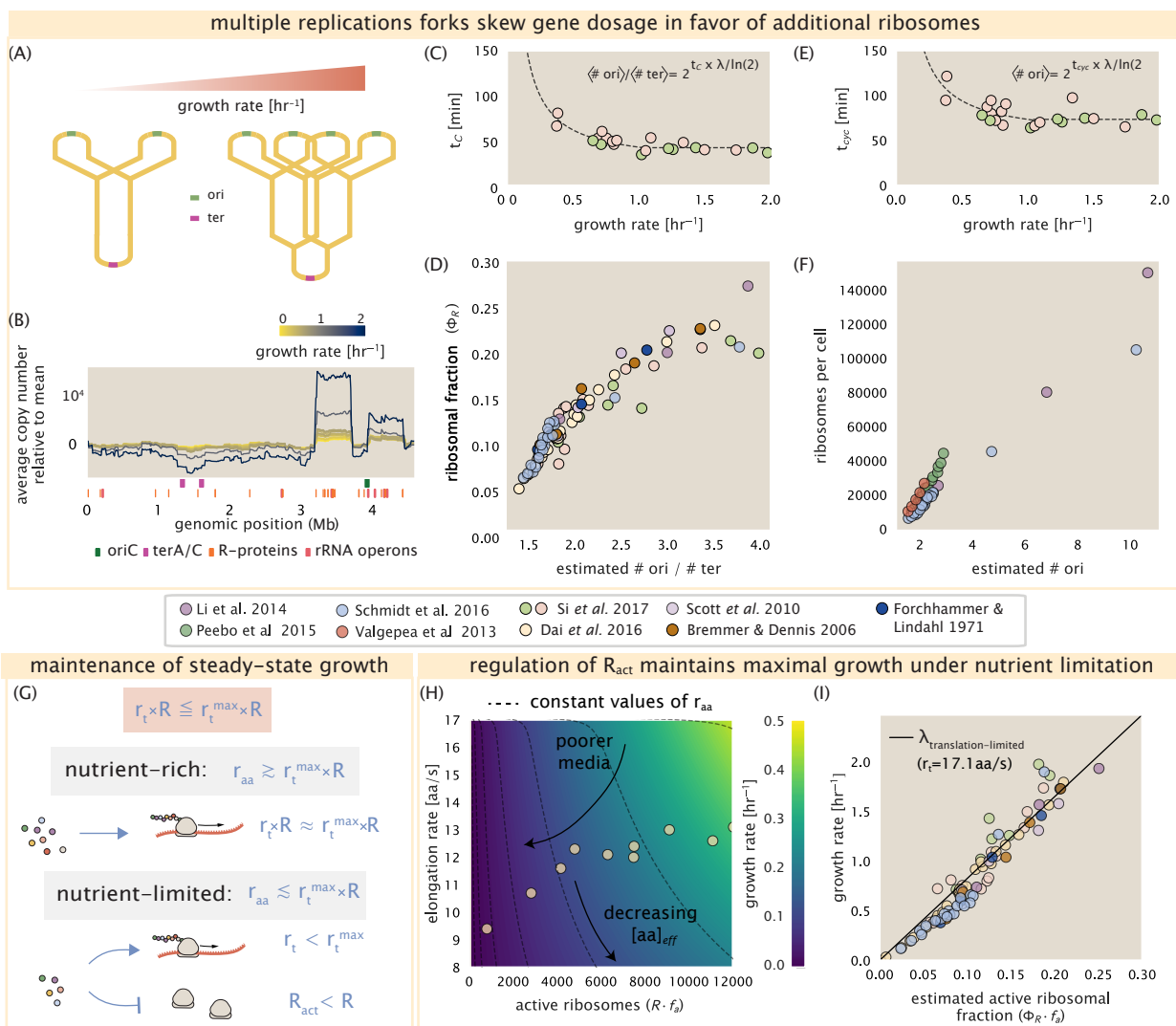


**Figure 4. Multiple replication forks skew gene dosage and ribosomal content.** (A) Schematic shows the expected increase in replication forks (or number of ori regions) as *E. coli* cells grow faster. (B) A running boxcar average of protein copy number is calculated for each each growth condition considered by Schmidt *et al.*. A 0.5 Mb averaging window was used. Protein copy numbers are reported relative to their condition-specific means in order to center all data sets. (C) and (E) show experimental data from Si *et al.* (2017) Solid lines show fits to the data, which were used to estimate  $\langle \# \text{ori} \rangle / \langle \# \text{ter} \rangle$  and  $\langle \# \text{ori} \rangle$  [NB: to note fit equations]. Red data points correspond to measurements in strain MG1655, while light green points are for strain NCM3722. (D) Plot compares our estimate of  $\langle \# \text{ori} \rangle / \langle \# \text{ter} \rangle$  to the experimental measurements of ribosomal abundance. Ribosomal fraction was approximated from the RNA/protein ratios of Dai *et al.* (2016) (yellow) and Si *et al.* (2017) (light red and light green) by the conversion RNA/protein ratio  $\approx \Phi_R \cdot 2.1$ . (F) Plot of the ribosome copy number estimated from the proteomic data against the estimated  $\langle \# \text{ori} \rangle$ . (G) Schematic showing translation-specific requirements for maintenance of steady-state growth. In a nutrient rich environment, amino acid supply  $r_{aa}$  is sufficiently in excess of demand by ribosomes translating at their maximal rate. In poorer nutrient conditions, reduced amino acid supply  $r_{aa}$  will decrease the rate of elongation. In a regime where  $r_{aa} < r_t \cdot R$ , the number of actively translating ribosomes will need to be reduced in order to maintain steady-state growth. (H) Translation elongation rate is plotted as a function of the number of actively translating ribosomes  $R \cdot f_a$ . Dashed lines correspond to a range of amino acid synthesis rates  $r_{aa}$ , from  $10^3$  to  $10^6$ . Growth rates are calculated according to Equation 1, assuming a constant ribosomal fraction of 8 percent. See appendix XX for additional details. (I) Experimental data from Dai *et al.* are used to estimate the fraction of actively translating ribosomes. The solid line represents the translation-limited growth rate for ribosomes elongating at 17.1 AA/s.

253 with our expectations, we find that ribosome copy number increases with the estimated  $\langle \# \text{ ori} \rangle$   
 254 (**Figure 4(F)**).

255 While it is difficult to distinguish between causality and correlation, the data is at least consistent  
 256 with the need for cells to increase their effective rRNA gene dosage in order to growth according  
 257 to the constraint set by Equation 2. These results may also shed some light on the notable in-  
 258 crease in ribosomal content that is observed when sublethal doses of antibiotics (??). Specifically,  
 259 if rRNA synthesis is rate limiting, and nutrient conditions largely dictate the extent of overlapping  
 260 DNA replication cycles, than addition of antibiotic will lengthen the doubling time and allow an  
 261 increase in the abundance of rRNA that can be synthesized relative to the rate of cell division. In  
 262 Supplemental Section XX, we consider this further using additional data from ?.

263 **Regulation of translating ribosomes helps maintain maximal growth according to  
 264 nutrient availability.**

265 While the above analysis provides a possible explanation for how *E. coli* can vary its ribosomal  
 266 content to maximize growth, it also presents a challenge in the limit of poorer nutrient conditions.  
 267 Recall from Equation 3 that ribosomal content should decrease to zero as growth decreases to zero.  
 268 While bacteria tend to decrease their ribosomal abundance in poorer nutrient conditions, they do  
 269 so only to some fixed, non-zero amount (??). Here we find a minimal ribosomal fraction of  $\approx 0.06$  in  
 270 the slowest growth conditions. From the perspective of a bacterium dealing with uncertain nutrient  
 271 conditions, there is likely a benefit for the cell to maintain some relative fraction of ribosomes to  
 272 support rapid growth as nutrient conditions improve.

273 The challenge however, lies in the cell's ability to maintain steady-state growth when ribosomes  
 274 are in excess of the rate that nutrients can be harvested and amino acids synthesized for consump-  
 275 tion **Figure 4G**. One explanation for this is that the elongation rate decreases in poorer growth con-  
 276 ditions. Cells, however, are still able to maintain a relatively high elongation rate even in stationary  
 277 phase ( $\approx 8 \text{ AA/s}$ , ??)). A second explanation is that there are mechanisms to regulate biological  
 278 activity in conditions of stress and nutrient-limitation; in particular through the small-molecule  
 279 alarmones (p)ppGpp (?). Here we explore these two observations to better understand their con-  
 280 sequence on growth rate.

281 We consider slow growth conditions ( $\lambda$  less than  $0.5 \text{ hr}^{-1}$ ) by assuming that the decrease in  
 282 elongation rate is due to a limiting supply of amino acids and a need for the cell to maintain excess  
 283 nutrients for cellular homeostasis under steady-state growth. There is some experimental support  
 284 showing that in poorer nutrient growth conditions, cells have lower amino acids concentrations  
 285 (?). We proceed by coarse graining the cell's amino acid supply as a single, effective rate-limiting  
 286 species (see Supplmental Section XX for a more complete discussion). Under such a scenario, the  
 287 elongation rate can described as simply depending on the maximum elongation rate ( $\approx 17.1 \text{ aa/s}$ ,  
 288 ??)), an effective  $K_d$ , and the limiting amino acid concentration  $[AA]_{eff}$ . Specifically, the elongation  
 289 rate is given by,

$$r_t = r_t^{max} \cdot \frac{1}{1 + K_d/[AA]_{eff}}. \quad (4)$$

290 For cells growing in minimal media + glucose, the amino acid concentration is of order 100 mM  
 291 (BNID: 110093, ??)). With a growth rate of about  $0.6 \text{ hr}^{-1}$  and elongation rate of 12.5 aa per second  
 292 (?), we can estimate an effective  $K_d$  of about 40 mM. Ultimately the steady state amino acid concen-  
 293 tration will depend on the difference between the supply of amino acids  $r_{aa}$  and consumption by  
 294 ribosomes  $r_t \cdot R \cdot f_a$ , where  $f_a$  accounts for the possible reduction of actively translating ribosomes.

295 In **Figure 4E** we consider how the maximal growth rate and elongation rates vary as a func-  
 296 tion of the number of actively translating ribosomes in this slow growth regime (see Supplemen-  
 297 tal Section XX for a complete description of the model). If we consider  $r_A A$  to be reflective of a  
 298 specific growth condition, by considering lines of constant  $r_A A$ , we find that cells grow fastest by  
 299 maximizing their fraction of actively translating ribosomes. When we consider the experimental

300 measurements from ?, we see that although cells indeed reduce  $R \times f_a$ , they do so in a way that  
 301 keeps  $[AA]_{eff}$  relatively constant. Given our estimate for the  $K_d$  of 40 mM, we would only expect  
 302 a decrease from 100 mM to about 35 mM in the slowest growth conditions. While experimental  
 303 data is limited, amino acid concentrations only decrease to about 60 mM for cells grown in minimal  
 304 media + acetate ( $\lambda = 0.3 \text{ hr}^{-1}$  in our proteomic data; value obtained from ?), qualitatively consistent  
 305 with our expectations.

306 Given the quantitative data from ?, which determined  $f_a$  across the entire range of growth  
 307 rates across our data, we next estimated the active fraction of ribosomal protein. As shown in  
 308 **Figure 4(G)**, we find that cells grow at a rate near the expected translation maximum expected from  
 309 Equation 1, using the maximum elongation rate of  $r_t = 17.1 \text{ aa per second}$ . This is in contrast to the  
 310 reality that ribosomes are translating at almost half this rate in the poorest growth conditions. This  
 311 highlights that there are alternative ways to grow according to the translated-limited growth rate  
 312 that is expected based with ribosomes translating at their maximal elongation rate. Specifically, it  
 313 is by adjusting  $r_t \times R' \times f_a \approx r_{tmax} \times R$  that cells are able to scale the growth limit set by Equation 2.

314 [NB, These observations will be very important to include in discussion section: A number of  
 315 recent papers highlight the possibility that (p)ppGpp may even provide a causal explanation for  
 316 the nutrient-limit scaling law. In the context of ribosomal activity, increased levels of (p)ppGpp are  
 317 associated with lower ribosomal content, and at slow growth appear to help reduce the fraction of  
 318 actively translating ribosomes (?). Titration of the cellular (p)ppGpp concentrations (up or down)  
 319 can invoke similar proteomic changes reminiscent of those observed under nutrient limitation (?).  
 320 In light of the limiting dependence of ribosome copy number on chromosomal gene dosage, it was  
 321 recently shown that growth in a (p)ppGpp null strain abolishes both the scaling in cell size and the  
 322  $\langle \# \text{ ori} \rangle / \langle \# \text{ ter} \rangle$  ratio. Instead, cells exhibited a high  $\langle \# \text{ ori} \rangle / \langle \# \text{ ter} \rangle$  closer to 4 and cell size more  
 323 consistent with a fast growth state where (p)ppGpp levels are low (?).]

## 324 References

- 325 Adelberg, G., Towbin, B. D., Rothschild, D., Dekel, E., Bren, A., and Alon, U. (2014). Hierarchy of non-glucose  
 326 sugars in *Escherichia coli*. *BMC Systems Biology*, 8(1):133.
- 327 Antonenko, Y. N., Pohl, P., and Denisov, G. A. (1997). Permeation of ammonia across bilayer lipid membranes  
 328 studied by ammonium ion selective microelectrodes. *Biophysical Journal*, 72(5):2187–2195.
- 329 Assentoft, M., Kaptan, S., Schneider, H.-P., Deitmer, J. W., de Groot, B. L., and MacAulay, N. (2016). Aquaporin 4  
 330 as a  $\text{NH}_3$  Channel. *Journal of Biological Chemistry*, 291(36):19184–19195.
- 331 Bauer, S. and Ziv, E. (1976). Dense growth of aerobic bacteria in a bench-scale fermentor. *Biotechnology and  
 332 Bioengineering*, 18(1):81–94. \_eprint: <https://onlinelibrary.wiley.com/doi/10.1002/bit.260180107>.
- 333 Belliveau, N. M., Barnes, S. L., Ireland, W. T., Jones, D. L., Sweredoski, M. J., Moradian, A., Hess, S., Kinney, J. B.,  
 334 and Phillips, R. (2018). Systematic approach for dissecting the molecular mechanisms of transcriptional  
 335 regulation in bacteria. *Proceedings of the National Academy of Sciences*, 115(21):E4796–E4805.
- 336 Bennett, B. D., Kimball, E. H., Gao, M., Osterhout, R., Van Dien, S. J., and Rabinowitz, J. D. (2009). Absolute  
 337 metabolite concentrations and implied enzyme active site occupancy in *Escherichia coli*. *Nature Chemical  
 338 Biology*, 5(8):593–599.
- 339 Booth, I. R., Mitchell, W. J., and Hamilton, W. A. (1979). Quantitative analysis of proton-linked transport systems.  
 340 The lactose permease of *Escherichia coli*. *Biochemical Journal*, 182(3):687–696.
- 341 Dai, X., Zhu, M., Warren, M., Balakrishnan, R., Okano, H., Williamson, J. R., Fredrick, K., and Hwa, T. (2018).  
 342 Slowdown of Translational Elongation in *Escherichia coli* under Hyperosmotic Stress. - PubMed - NCBI. *mBio*,  
 343 9(1):281.
- 344 Dai, X., Zhu, M., Warren, M., Balakrishnan, R., Patsalo, V., Okano, H., Williamson, J. R., Fredrick, K., Wang, Y.-P.,  
 345 and Hwa, T. (2016). Reduction of translating ribosomes enables *Escherichia coli* to maintain elongation rates  
 346 during slow growth. *Nature Microbiology*, 2(2):16231.

- 347 Escalante, A., Salinas Cervantes, A., Gosset, G., and Bolívar, F. (2012). Current knowledge of the *Escherichia coli*  
 348 phosphoenolpyruvate-carbohydrate phosphotransferase system: Peculiarities of regulation and impact on  
 349 growth and product formation. *Applied Microbiology and Biotechnology*, 94(6):1483–1494.
- 350 Feist, A. M., Henry, C. S., Reed, J. L., Krummenacker, M., Joyce, A. R., Karp, P. D., Broadbelt, L. J., Hatzimanikatis,  
 351 V., and Palsson, B. Ø. (2007). A genome-scale metabolic reconstruction for *Escherichia coli* K-12 MG1655 that  
 352 accounts for 1260 ORFs and thermodynamic information. *Molecular Systems Biology*, 3(1):121.
- 353 Fernández-Coll, L., Maciąg-Dorszynska, M., Tailor, K., Vadia, S., Levin, P. A., Szalewska-Palasz, A., Cashel, M.,  
 354 and Dunny, G. M. (2020). The Absence of (p)ppGpp Renders Initiation of *Escherichia coli* Chromosomal DNA  
 355 Synthesis Independent of Growth Rates. *mBio*, 11(2):45.
- 356 Gama-Castro, S., Salgado, H., Santos-Zavaleta, A., Ledezma-Tejeida, D., Muñiz-Rascado, L., García-Sotelo, J. S.,  
 357 Alquicira-Hernández, K., Martínez-Flores, I., Pannier, L., Castro-Mondragón, J. A., Medina-Rivera, A., Solano-  
 358 Lira, H., Bonavides-Martínez, C., Pérez-Rueda, E., Alquicira-Hernández, S., Porrón-Sotelo, L., López-Fuentes,  
 359 A., Hernández-Koutoucheva, A., Moral-Chávez, V. D., Rinaldi, F., and Collado-Vides, J. (2016). RegulonDB  
 360 version 9.0: High-level integration of gene regulation, coexpression, motif clustering and beyond. *Nucleic  
 361 Acids Research*, 44(D1):D133–D143.
- 362 Harris, L. K. and Theriot, J. A. (2018). Surface Area to Volume Ratio: A Natural Variable for Bacterial Morphogenesis. *Trends in microbiology*, 26(10):815–832.
- 364 Harris, R. M., Webb, D. C., Howitt, S. M., and Cox, G. B. (2001). Characterization of PitA and PitB from *Escherichia  
 365 coli*. *Journal of Bacteriology*, 183(17):5008–5014.
- 366 Heldal, M., Norland, S., and Tumyr, O. (1985). X-ray microanalytic method for measurement of dry matter and  
 367 elemental content of individual bacteria. *Applied and Environmental Microbiology*, 50(5):1251–1257.
- 368 Hui, S., Silverman, J. M., Chen, S. S., Erickson, D. W., Basan, M., Wang, J., Hwa, T., and Williamson, J. R. (2015).  
 369 Quantitative proteomic analysis reveals a simple strategy of global resource allocation in bacteria. *Molecular  
 370 Systems Biology*, 11(2):e784–e784.
- 371 Ireland, W. T., Beeler, S. M., Flores-Bautista, E., Belliveau, N. M., Sweredoski, M. J., Moradian, A., Kinney, J. B.,  
 372 and Phillips, R. (2020). Deciphering the regulatory genome of *Escherichia coli*, one hundred promoters at a  
 373 time. *bioRxiv*.
- 374 Jacob, F. and Monod, J. (1961). Genetic regulatory mechanisms in the synthesis of proteins. *Journal of Molecular  
 375 Biology*, 3(3):318–356.
- 376 Jun, S., Si, F., Pugatch, R., and Scott, M. (2018). Fundamental principles in bacterial physiology - history, recent  
 377 progress, and the future with focus on cell size control: A review. *Reports on Progress in Physics*, 81(5):056601.
- 378 Khademi, S., O'Connell, J., Remis, J., Robles-Colmenares, Y., Miercke, L.J.W., and Stroud, R. M. (2004). Mechanism  
 379 of Ammonia Transport by Amt/MEP/Rh: Structure of AmtB at 1.35 Å. *Science*, 305(5690):1587–1594.
- 380 Li, G.-W., Burkhardt, D., Gross, C., and Weissman, J. S. (2014). Quantifying absolute protein synthesis rates  
 381 reveals principles underlying allocation of cellular resources. *Cell*, 157(3):624–635.
- 382 Liebermeister, W., Noor, E., Flamholz, A., Davidi, D., Bernhardt, J., and Milo, R. (2014). Visual account of protein  
 383 investment in cellular functions. *Proceedings of the National Academy of Sciences*, 111(23):8488–8493.
- 384 Liu, M., Durfee, T., Cabrera, J. E., Zhao, K., Jin, D. J., and Blattner, F. R. (2005). Global Transcriptional Programs  
 385 Reveal a Carbon Source Foraging Strategy by *Escherichia coli*. *Journal of Biological Chemistry*, 280(16):15921–  
 386 15927.
- 387 Maaløe, O. (1979). *Regulation of the Protein-Synthesizing Machinery—Ribosomes, tRNA, Factors, and So On. Gene  
 388 Expression*. Springer.
- 389 Milo, R., Jorgensen, P., Moran, U., Weber, G., and Springer, M. (2010). BioNumbers—the database of key num-  
 390 bers in molecular and cell biology. *Nucleic Acids Research*, 38(suppl\_1):D750–D753.
- 391 Monod, J. (1947). The phenomenon of enzymatic adaptation and its bearings on problems of genetics and  
 392 cellular differentiation. *Growth Symposium*, 9:223–289.
- 393 Neidhardt, F. C., Ingraham, J., and Schaechter, M. (1991). *Physiology of the Bacterial Cell - A Molecular Approach*,  
 394 volume 1. Elsevier.

- 395 Peebo, K., Valgepea, K., Maser, A., Nahku, R., Adamberg, K., and Vilu, R. (2015). Proteome reallocation in *Escherichia coli* with increasing specific growth rate. *Molecular BioSystems*, 11(4):1184–1193.
- 396
- 397 Phillips, R. (2018). Membranes by the Numbers. In *Physics of Biological Membranes*, pages 73–105. Springer, Cham, Cham.
- 398
- 399 Ramos, S. and Kaback, H. R. (1977). The relation between the electrochemical proton gradient and active trans-  
400 port in *Escherichia coli* membrane vesicles. *Biochemistry*, 16(5):854–859.
- 401 Rosenberg, H., Gerdes, R. G., and Chegwidden, K. (1977). Two systems for the uptake of phosphate in *Escherichia coli*. *Journal of Bacteriology*, 131(2):505–511.
- 402
- 403 Schaechter, M., Maaløe, O., and Kjeldgaard, N. O. (1958). Dependency on Medium and Temperature of Cell Size  
404 and Chemical Composition during Balanced Growth of *Salmonella typhimurium*. *Microbiology*, 19(3):592–606.
- 405 Schmidt, A., Kochanowski, K., Vedelaar, S., Ahrné, E., Volkmer, B., Callipo, L., Knoops, K., Bauer, M., Aebersold,  
406 R., and Heinemann, M. (2016). The quantitative and condition-dependent *Escherichia coli* proteome. *Nature Biotechnology*, 34(1):104–110.
- 407
- 408 Scholz, S. A., Diao, R., Wolfe, M. B., Fivenson, E. M., Lin, X. N., and Freddolino, P. L. (2019). High-Resolution  
409 Mapping of the *Escherichia coli* Chromosome Reveals Positions of High and Low Transcription. *Cell Systems*,  
410 8(3):212–225.e9.
- 411 Scott, M., Gunderson, C. W., Mateescu, E. M., Zhang, Z., and Hwa, T. (2010). Interdependence of cell growth and  
412 gene expression: origins and consequences. *Science*, 330(6007):1099–1102.
- 413 Sekowska, A., Kung, H.-F., and Danchin, A. (2000). Sulfur Metabolism in *Escherichia coli* and Related Bacteria:  
414 Facts and Fiction. *Journal of Molecular Microbiology and Biotechnology*, 2(2):34.
- 415 Si, F., Le Treut, G., Sauls, J. T., Vadia, S., Levin, P. A., and Jun, S. (2019). Mechanistic Origin of Cell-Size Control  
416 and Homeostasis in Bacteria. *Current Biology*, 29(11):1760–1770.e7.
- 417 Si, F., Li, D., Cox, S. E., Sauls, J. T., Azizi, O., Sou, C., Schwartz, A. B., Erickstad, M. J., Jun, Y., Li, X., and Jun, S. (2017).  
418 Invariance of Initiation Mass and Predictability of Cell Size in *Escherichia coli*. *Current Biology*, 27(9):1278–1287.
- 419 Sirko, A., Zatyka, M., Sadowy, E., and Hulanicka, D. (1995). Sulfate and thiosulfate transport in *Escherichia coli* K-  
420 12: Evidence for a functional overlapping of sulfate- and thiosulfate-binding proteins. *Journal of Bacteriology*,  
421 177(14):4134–4136.
- 422 Stasi, R., Neves, H. I., and Spira, B. (2019). Phosphate uptake by the phosphonate transport system PhnCDE.  
423 *BMC Microbiology*, 19.
- 424 Szenk, M., Dill, K. A., and de Graff, A. M. R. (2017). Why Do Fast-Growing Bacteria Enter Overflow Metabolism?  
425 Testing the Membrane Real Estate Hypothesis. *Cell Systems*, 5(2):95–104.
- 426 Taheri-Araghi, S., Bradde, S., Sauls, J. T., Hill, N. S., Levin, P. A., Paulsson, J., Vergassola, M., and Jun, S. (2015).  
427 Cell-size control and homeostasis in bacteria. - PubMed - NCBI. *Current Biology*, 25(3):385–391.
- 428 Taymaz-Nikerel, H., Borujeni, A. E., Verheijen, P. J. T., Heijnen, J. J., and van Gulik, W. M. (2010).  
429 Genome-derived minimal metabolic models for *Escherichia coli* mg1655 with estimated in vivo  
430 respiratory ATP stoichiometry. *Biotechnology and Bioengineering*, 107(2):369–381. \_eprint:  
431 <https://onlinelibrary.wiley.com/doi/pdf/10.1002/bit.22802>.
- 432 Valgepea, K., Adamberg, K., Seiman, A., and Vilu, R. (2013). *Escherichia coli* achieves faster growth by increasing  
433 catalytic and translation rates of proteins. *Molecular BioSystems*, 9(9):2344.
- 434 van Heeswijk, W. C., Westerhoff, H. V., and Boogerd, F. C. (2013). Nitrogen Assimilation in *Escherichia coli*: Putting  
435 Molecular Data into a Systems Perspective. *Microbiology and Molecular Biology Reviews*, 77(4):628–695.
- 436 Willsky, G. R., Bennett, R. L., and Malamy, M. H. (1973). Inorganic Phosphate Transport in *Escherichia coli*: Involvement  
437 of Two Genes Which Play a Role in Alkaline Phosphatase Regulation. *Journal of Bacteriology*, 113(2):529–  
438 539.
- 439 Zhang, L., Jiang, W., Nan, J., Almqvist, J., and Huang, Y. (2014a). The *Escherichia coli* CysZ is a pH dependent sulfate  
440 transporter that can be inhibited by sulfite. *Biochimica et Biophysica Acta (BBA) - Biomembranes*, 1838(7):1809–  
441 1816.

- 442** Zhang, Z., Aboulwafa, M., and Saier, M. H. (2014b). Regulation of crp gene expression by the catabolite repres-  
**443** sor/activator, cra, in *Escherichia coli*. *Journal of Molecular Microbiology and Biotechnology*, 24(3):135–141.
- 444** Zhu, M. and Dai, X. (2019). Growth suppression by altered (p)ppGpp levels results from non-optimal resource  
**445** allocation in *Escherichia coli*. *Nucleic Acids Research*, 47(9):4684–4693.